Chemosphere 208 (2018) 595–605

Contents lists available at ScienceDirect

Chemosphere

journal homepage: www.elsevier.com/locate/chemosphere

Synthesis of nanostructured titanium dioxide layer onto kaolin hollow fibre membrane via hydrothermal method for decolourisation of reactive black 5

Nur Hamizah Mohtor [a], Mohd Hafiz Dzarfan Othman [a, *], Suriani Abu Bakar [b], Tonni Agustiono Kurniawan [c], Hazlini Dzinun [a, d], Muhammad Noorul Anam Mohd Norddin [a], Zanariah Rajis [a]

[a] Advanced Membrane Technology Research Centre (AMTEC), Universiti Teknologi Malaysia, 81310 Skudai, Johor, Malaysia
[b] Nanotechnology Research Centre, Department of Physics, Faculty of Science and Mathematics, Universiti Pendidikan Sultan Idris, 35900 Tanjung Malim, Perak, Malaysia
[c] Key Laboratory of the Ministry of Education for Coastal and Wetland Ecosystems, College of Ecology and the Environment, Xiamen University, Xiamen 361102 Fujian, PR China
[d] Department of Science and Mathematics, Centre for Diploma Studies, Universiti Tun Hussein Onn Malaysia, 84600 Muar, Johor, Malaysia

HIGHLIGHTS

- This study emphasized on the use of kaolin as the support for the TiO_2 nanorods layer.
- Hydrothermal reaction times of TiO_2 were varied from 2 to 10 h and brought significant impacts on its properties.
- The well-dispersed of TiO_2 nanorods have improved the surface affinity of membrane towards water.
- Kaolin/TNR membrane with 10 h of reaction time exhibited the highest water permeation of 165 L/h.m^2.bar.
- The prepared membrane showed the highest photocatalytic activity of 80.3% in the dye decolorization.

ARTICLE INFO

Article history:
Received 10 April 2018
Accepted 26 May 2018
Available online 28 May 2018

Handling Editor: Y. Yeomin Yoon

Keywords:
Hydrothermal method
kaolin/TNR membrane
Photocatalytic degradation

ABSTRACT

Hydrothermal method has been proven to be an effective method to synthesise the nanostructured titanium dioxide (TiO_2) with good morphology and uniform distribution at low temperature. Despite of employing a well-known and commonly used glass substrate as the support to hydrothermally synthesise the nanostructured TiO_2, this study emphasised on the application of kaolin hollow fibre membrane as the support for the fabrication of kaolin/TiO_2 nanorods (TNR) membrane. By varying the hydrothermal reaction times (2 h, 6 h, and 10 h), the different morphology, distribution, and properties of TiO_2 nanorods on kaolin support were observed by field emission scanning electron microscopy (FESEM), energy-dispersive X-ray spectroscopy (EDX), atomic force microscope (AFM), X-ray diffraction (XRD) and Fourier transform infrared spectroscopy (FTIR). It was found that the well-dispersed of TiO_2 nanorods have improved the surface affinity of kaolin/TNR membrane towards water, allowing kaolin/TNR membrane prepared from 10 h of hydrothermal reaction to exhibit the highest water permeation of 165 L/h.m^2.bar. In addition, this prepared membrane also showed the highest photocatalytic activity of 80.3% in the decolourisation of reactive black 5 (RB5) under UV irradiation. On top of that, the kaolin/TNR membrane prepared from 10 h of hydrothermal reaction also exhibited a good resistance towards photocorrosion, enabling the reuse of this membrane for three consecutive cycles of photocatalytic degradation of RB5 without showing significant reduction in photocatalytic efficiency towards the decolourisation of RB5.

1. Introduction

Research on water and wastewater treatment by using various semiconductor photocatalyses driven by light is well explored and

* Corresponding author.
E-mail address: hafiz@petroleum.utm.my (M.H.D. Othman).

https://doi.org/10.1016/j.chemosphere.2018.05.159
0045-6535/

not something new. Although various semiconductors (as well as their composites) have been investigated as photocatalysts for photocatalytic degradation of aqueous pollutants, titanium dioxide (TiO_2) remains as the most widely studied and employed photocatalyst since it is commercially available, inexpensive, non-toxic and chemically stable (Leong et al., 2014). The advancement in research nowadays has made the nanostructured TiO_2 such as nanorods, nanotubes, nanowires and nanoflowers as an alternative to nanoparticles TiO_2. In comparison to nanoparticles TiO_2, the nanostructured TiO_2 has been proven to possess outstanding photochemical, electrical, and optical properties that resulted in gaining significant interest for several applications including photocatalysis (Linsebigler et al., 1995), photosensors (Okuya et al., 2004), and photovoltaics (Xiong et al., 2015).

Due to the promising potentials of nanostructured TiO_2 in various applications, various methods have been attempted by researchers in order to synthesise the desired nanostructured TiO_2 with high surface area-to-volume ratio, including hydrothermal method (Yuan and Su, 2004), sol-gel process (Song et al., 2005), chemical vapour deposition (Chang et al., 2009) and template-assisted method (Jiu et al., 2004). Among these methods, hydrothermal method has been selected as one of the most promising methods that can fabricate the homogenous nanostructured TiO_2 in the stable temperature and pressure. Previous studies have successfully fabricated various forms of nanostructured TiO_2 such as nanorods and nanoflowers (Ahmad et al., 2016a), nanotubes (Subramaniam et al., 2017), and nanowires (Faisal, 2015) by using this simple, yet reliable and cost effective method. Thus, by aiming to prepare the homogeneous thin film of nanostructured TiO_2 in fast but low cost approach, hydrothermal method has been chosen to be utilised in this study.

In the scope of immobilisation of TiO_2 on the substrate or support, previous researchers, who employed hydrothermal method in their works, commonly used fluorine-doped tin oxide (FTO) coated glass substrate in order to synthesise the desired nanostructured TiO_2 on the surface of glass substrate (Tao et al., 2016; Yusoff et al., 2016). However, this study have been attempted to use the kaolin hollow fibre membrane as the ceramic membrane support with hollow fibre morphology, rather than well-known FTO glass substrate with flat surface. The handful cleaning step of FTO glass substrate during the preparation of hydrothermal process can be eliminated when kaolin hollow fibre membrane was used instead. In addition, the kaolin hollow fibre membrane was fabricated using Malaysian kaolin powder as its sole low cost ceramic material (Mohtor et al., 2017), making it as an economical choice for ceramic membrane support, which is in line with the cost effective of hydrothermal method.

The application of alumina as a well-known ceramic material for the preparation of ceramic membrane may be replaced by kaolin since the applied sintering temperature for ceramic membrane can be decreased from 1600 °C (for alumina membrane) to 1250 °C (for kaolin membrane) and the production cost may be reduced as the price of kaolin is about 100 times cheaper than that of alumina (Harabi et al., 2014). In addition, this work focused on the application of kaolin membrane in hollow fibre configuration that possesses a high surface area-to-volume ratio in comparison to other membrane configurations of kaolin membrane such as flat sheet (Sarbatly, 2011) and tubular (Bouzerara et al., 2006). Thus, the kaolin hollow fibre membrane can be considered as a suitable candidate for TiO_2 support as it has good mechanical strength and high surface area-to-volume ratio (Mohtor et al., 2017) that are essential for ensuring the TiO_2 layer to be able to withstand the pressure applied over the entire membrane and maintain the high photocatalytic activity of TiO_2 through maximum illumination of light source to the surface of TiO_2.

TiO_2 has three well-known crystalline phases, which are anatase phase (tetragonal), rutile phase (tetragonal), and brookite phase (orthorhombic). Among these, rutile is high temperature stable phase, while anatase and brookite are metastable phase, which can be transformed into rutile phase when treated at high temperature (Ahmad et al., 2016b). Rutile-phased TiO_2 nanorods and nanoflowers, which hydrothermally grew on FTO-coated glass substrate were successfully suited for sensor devices application (Cao et al., 2011) and dye-sensitized solar cell application (Zhang et al., 2010). Although there was only a few works on rutile-phased TiO_2 nanorods or nanoflowers for photocatalytic degradation of pollutants (Tao et al., 2016; Mohamed et al., 2016), rutile-phased TiO_2 has also been proven to be suited for photocatalytic application. So, this study was conducted to determine the photocatalytic efficiency of kaolin/TNR membrane in colour degradation of dye under UV irradiation.

Various types of dye have been successfully degraded using TiO_2 under ultraviolet (UV) exposure. In this study, Reactive Black 5 (RB5) was chosen as a model compound of azo (R-N=N-R′) dye to be degraded under UV irradiation. Since RB5 is a diazo dye, it has two azo double bonds (R-N=N-R') with four aromatic systems, which makes this type of dye recalcitrant in the environment as breakdown of diazo bonds is more difficult from its counterpart of mono-azo type. Damodar et al. (2009) and Lin et al. (2012) reported that RB5 have been successfully to be degraded with 100% of colour removal efficiency only under UVC illumination using immobilised TiO_2. Due to the harmful UVC light exposure towards the environment and public health, this study has selected UVA lamp as the source of UV light for the photocatalytic degradation of RB5 using kaolin/TNR hollow fibre membrane.

2. Experimental

2.1. Materials

Kaolin powder with an average particle size of 2–4 μm (KM55, Kaolin (Malaysia) Sdn. Bhd.), polyethersulfone (PES) (Veradel® A-301, Solvay Advanced Polymers), polyethylene glycol 30-dipolyhydroxystrearate (Arlacel P135, Uniqema), and *N*-methyl-2-pyrrolidone (NMP) (AR grade, Merck) were used as the ceramic particle, polymer binder, dispersant, and solvent, respectively, for the preparation of ceramic suspension. In addition, tap water was used as the internal and external coagulants during the extrusion process of ceramic suspension. On the other hand, concentrated hydrochloric acid (36.5–38.0% HCl) (AR grade, J. T. Baker), deionized (DI) water, and titanium tetrabutoxide (TBOT) (AR grade, Sigma-Aldrich) were consumed in the hydrothermal reaction. For the photocatalytic degradation of dye, RB5 (dye content ≥50%, Sigma-Aldrich) was selected as the diazo dye that needed to be degraded under UV irradiation.

2.2. Fabrication of kaolin hollow fibre membrane

For the preparation of kaolin hollow fibre membrane, there were basically two main steps involved which were extrusion and sintering processes. Prior to the extrusion process, the ceramic suspension consisted of kaolin powder (40 wt%), PES (5 wt%), NMP (54 wt%) and Arlacel P135 (1 wt%) should be prepared first and the preparation steps were explained elsewhere (Mohtor et al., 2017). The extrusion process was carried out by applying the dry/wet phase inversion technique, in which the degassed ceramic suspension (flow rate of 9 mL/min) was extruded simultaneously with the internal coagulant (flow rate of 10 mL/min) through tube-in-orifice spinneret (ID 1.2 m, OD 2.8 mm), directly into the external

coagulant bath with the air gap of 5 cm. The formed kaolin precursor was then dried at room temperature after completing the phase inversion process by immersion in the external coagulation bath for about 24 h. Finally, in order to obtain the final kaolin hollow fibre membrane, the dried kaolin precursor was sintered at target temperature of 1350 °C in tubular furnace (Brand: Magna value, Model: XL-1700) using the same sintering profile from our previous work (Mohtor et al., 2017). The obtained kaolin hollow fibre membrane was finally used as the kaolin support for the deposition of TiO_2 nanorods on the outer membrane surface for the preparation of kaolin/TNR membrane.

2.3. Preparation of kaolin/TNR membrane

With the aim to prepare kaolin/TNR membrane, the hydrothermal method was utilised by firstly preparing a chemical solution, which consisted of 120 mL of concentrated HCl that was added into 120 mL of DI water, followed by vigorous stirring using magnetic stirrer (Brand: Thermo Scientific) for about 10 min. Then, 6 mL of TBOT was added dropwise into the solution, followed by another 10 min of stirring in order to obtain the final transparent solution. Prior to the hydrothermal process, 10 hollow fibres of kaolin support with both sealed ends were placed inside the steel-made autoclave with Teflon-made liner before adding the resultant solution. As illustrated in Fig. 1, the hydrothermal process was carried out at 150 °C in an oven (Brand: Memmert) for different reaction times (2 h, 6 h, and 10 h). By using the advantage of ceramic membrane in the application that required the high temperature and pressure conditions, the kaolin support that was sintered at 1350 °C with mechanical strength of 52 MPa was suitable to be submerged in the reaction solution inside the autoclave without being dissolved or broken apart throughout the hydrothermal process. Upon the completion of hydrothermal process, the autoclave was taken out from the oven and cooled down to ambient temperature. Lastly, the prepared kaolin/TNR membranes were taken out from the autoclave and rinsed thoroughly with DI water several times before letting them to completely dry at ambient temperature.

2.4. Characterisations

The morphology and distribution of TiO_2 nanorods on the outer membrane surface of kaolin support were observed by field emission scanning electron microscope (FESEM) (Brand: Hitachi, Model: SU8020) and their elemental distribution was analysed by energy dispersive X-ray (EDX) spectrometer (Brand: Oxford Instruments, Model: X-Max) using mapping that were drawn across the sample surface. From FESEM image of the surface of membrane, the length and diameter of TiO_2 nanorods were measured in which the average length and diameter of TiO_2 nanorods were calculated based on ten measurements taken for each membrane sample. For sample preparation, the membrane was fractured to obtain the neat cut of its cross-section and placed on metal holder before being sputter-coated with gold under vacuum for 3 min. Meanwhile, the surface roughness of membrane was analysed by atomic force microscope (AFM) (Brand: Park System, Model: XE-100). For sample preparation, the membrane was cut into small pieces and attached to the sample holder. AFM micrographs were obtained by scanning on the membrane surface with the area of 10 μm × 10 μm using the sharp tip at the end of cantilever.

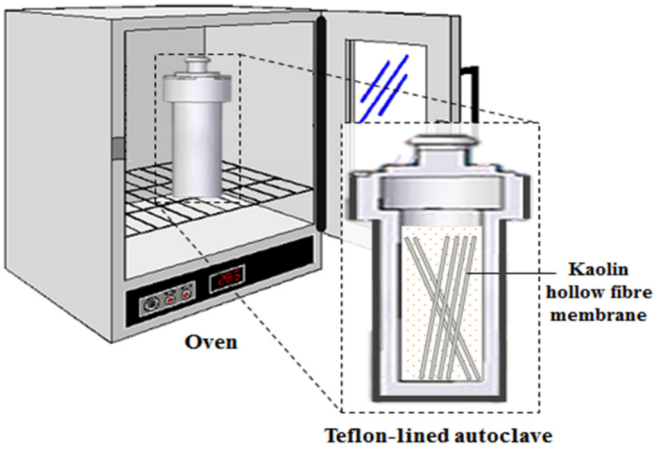

Fig. 1. Schematic diagram of hydrothermal process setup.

The presence of crystalline phase of TiO_2 on the outer surface of prepared membrane was detected by X-ray diffractometer (XRD) (Brand: Bruker D8 Advance, Model: D8-02/01–378) with CuKα radiation for obtaining the XRD patterns in the range of $10 \leq 2\theta$ (°) ≤ 70 at 1° scan rate. On the other hand, the determination of changes in functional groups of both kaolin support and kaolin/TNR membrane was analysed by attenuated total reflection (ATR) mode using Fourier transform infrared (FTIR) spectrometer (Brand: Thermo Nicolet Corporation, Model: Nicolet 5700) in order to record the FTIR spectra in the region of 4000–600 cm^{-1} at ambient temperature. Meanwhile, the hydrophilicity of membrane was characterised by contact angle measurement that was measured using contact angle goniometer (Brand: Dataphysics, Model: OCA 15 EC). By using sessile drop method and DI water as its contact droplet, the constant dosing volume of 0.5 μL of droplet was slowly placed on the dried membrane surface and its contact angle was measured. The average contact angle was calculated based on ten measurements that was obtained from different spots on the membrane surface for each membrane sample. In the measurement of water contact angle, the solid surface was considered as hydrophilic when the contact angle <90°, while >90° indicated the solid surface as hydrophobic (Dzinun et al., 2015).

For water permeation test, the ultrafiltration system in the cross-flow filtration mode was used in order to conduct the filtration at pressure of 1 bar and temperature of 25 °C by using the membrane with approximately 2 cm of length. Prior to any measurement, the steady state flux needs to be obtained first by compacting the membrane with water as the feed at pressure of 1.5 bar for about 30 min. The water permeation of membrane was calculated by using:

$$L_p = \frac{\Delta V}{A_m \, \Delta t \, \Delta P} \quad (1)$$

where L_p is the water permeation ($L/m^2.h.bar$), ΔV is the volume of water permeated through membrane (L), A_m is the effective membrane area (m^2), Δt is the permeation time (h) and ΔP is the transmembrane pressure (bar). The average water permeation was measured from three measurements taken for each membrane sample.

2.5. Photocatalytic degradation of RB5

The photocatalytic performance of kaolin/TNR membrane was studied by using RB5 as a surrogate indicator for evaluating the photocatalytic efficiency of kaolin/TNR membrane in decolourisation of dye under UV irradiation. As illustrated in Fig. 2, the photocatalytic degradation of RB5 was performed in the batch membrane photoreactor using a membrane module that fitted with 10 hollow fibres of kaolin/TNR membrane with sealed both ends

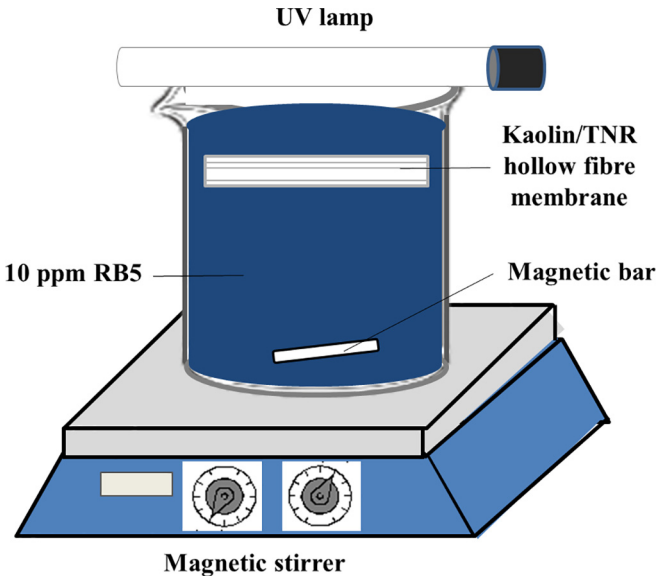

Fig. 2. Schematic diagram of photocatalytic test setup.

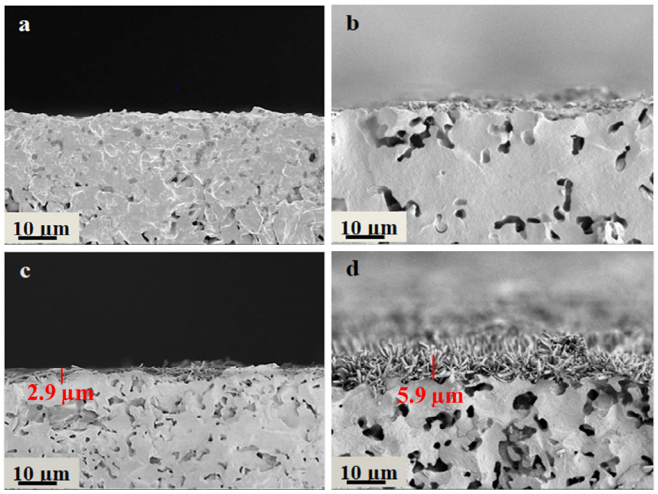

Fig. 3. FESEM images of the cross-sectional of (a) kaolin support and kaolin/TNR membrane that prepared at (b) 2 h, (c) 6 h, and (d) 10 h of reaction time.

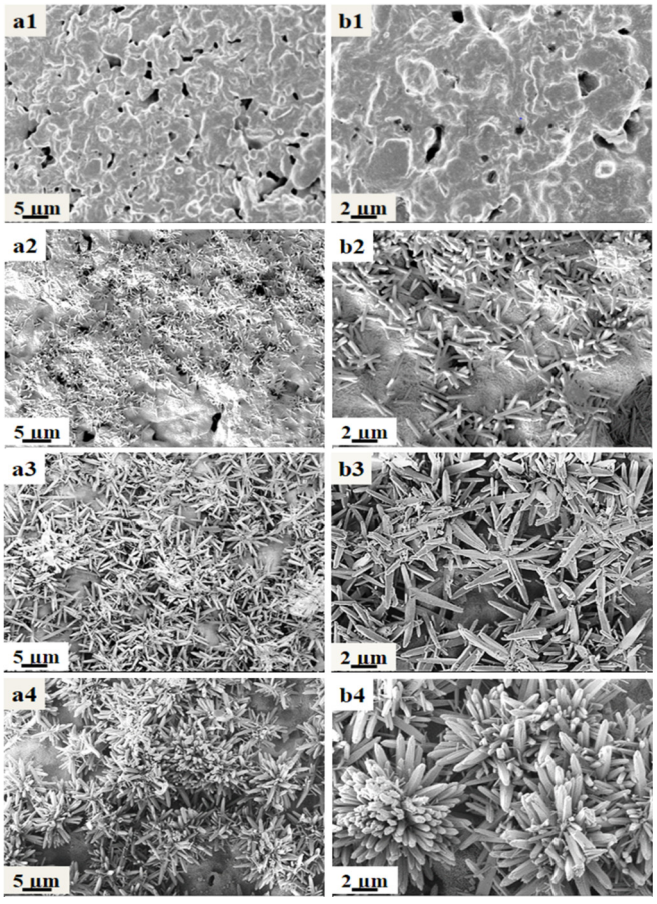

Fig. 4. FESEM images of the outer membrane surface at different magnifications of (a) 2k x and (b) 5k x of (1) kaolin support and kaolin/TNR membrane that prepared at (2) 2 h, (3) 6 h, and (4) 10 h of reaction time.

(exposed membrane length: 8 cm; total effective membrane area: 40 cm^2) that submerged in magnetic stirred 500 mL of 10 ppm RB5 solution as the feed solution. Prior to the photocatalytic process, the feed solution was stirred for 100 min in the dark at 25 °C in order to ensure that the photocatalytic reaction was conducted after achieving the adsorption-desorption equilibrium. By fixing the distance between membrane and UV light source at 5 cm, 36 W UVA lamp (Brand: Philips, Japan) was used to irradiate the immobilised TiO_2 on kaolin support by emitting radiation at 365 nm of wavelength when it was turned on. In order to prevent the escape of harmful UV light, the glass container was fully covered with aluminium foils.

Throughout the photocatalytic process, 1.5 mL of feed solution was collected at specific time intervals of 1 h, where the absorbance value of the sample solution was measured by using UV–Visible spectrophotometer (Brand: Hach Company, Model: DR5000) at an absorbance wavelength of 597 nm. The concentration of RB5 in the feed solution during the photocatalytic process was calculated based on the calibration curve obtained from the absorbance value of RB5 solution at 597 nm of wavelength. By obtaining the concentration of RB5, RB5 degradation, η (%) was calculated as follows:

$$\eta = \frac{C_o - C_t}{C_o} \times 100 \quad (2)$$

where C_0 is the initial concentration of dye solution, while C_t is the concentration of dye solution after photocatalytic degradation at specific time interval.

3. Results and discussion

3.1. Morphological properties of membrane

The effect of different hydrothermal reaction times on the distribution and morphology of TiO_2 on kaolin support were examined by FESEM. Their FESEM images of the cross-sectional and outer membrane surface at different magnifications were presented in Figs. 3 and 4, respectively. As revealed by the FESEM image of the cross-sectional of kaolin support in Fig. 3 **(a)**, the membrane structure comprised of sponge-like structure near the outer membrane surface, which functioned as the separation layer for kaolin support. The formation of TiO_2 layer on the kaolin support basically did not impose any changes on the overall cross-sectional structure of kaolin support, indicating that the deposition of TiO_2 only took place on the outer membrane surface of kaolin support, as observed in Fig. 3 **(b)**, **(c)**, and **(d)**. From Fig. 3 **(b)**, there was no

continuous formation of TiO_2 layer found on the outer membrane surface when the hydrothermal reaction conducted for 2 h. This observation was predicted due to the fact that the shortest duration of hydrothermal reaction was only able to produce a small amount of TiO_2 on the outer membrane surface, resulting in the absence of TiO_2 layer with measurable thickness. However, by increasing the period of time used for hydrothermal process into 6 h and 10 h, the incline in the amount of synthesised TiO_2 on the outer membrane surface was perceived. As a result, the uniform TiO_2 layer was successfully formed and seen on the outer membrane surface with different thickness of 2.9 μm in Figs. 3 **(c)** and 5.9 μm in Fig. 3 **(d)**, when 6 h and 10 h of reaction times were utilised for hydrothermal process, respectively.

On the other hand, the FESEM images of the outer membrane surface of neat membrane and its coated counterparts were presented in Fig. 4. As shown in Fig. 4 **(a1) and (b1)**, the outer membrane surface of kaolin support was consisted of microporous structure with interconnected, plate-like grains and irregular pores. By carrying out the hydrothermal reaction for 2 h, the outer membrane surface was randomly deposited with TiO_2 in nanorod form as depicted in Fig. 4 **(a2)** and thus, the prepared membrane could be denoted as kaolin/TiO_2 nanorods (TNR) membrane. The random deposition of TiO_2 nanorods on some parts of the outer membrane surface was due to the insufficient time for the outer membrane surface to be uniformly distributed with TiO_2 nanorods. Meanwhile, the FESEM image of the outer membrane surface at higher magnification in Fig. 4 **(b2)** revealed that the TiO_2 nanorods were in slanting position with an average diameter of 0.34 μm and an average length of 2.26 μm. The observation was in contrast to the work conducted by Tao et al. (2016) as their TiO_2 nanorods were hydrothermally formed in perpendicular to the fluorine-doped tin oxide (FTO)-coated glass substrate, owing to the presence of flat surface of glass substrate that easily promoted the formation of vertically-aligned TiO_2 nanorods with uniform distribution. Thus, the formation of slanted TiO_2 nanorods with random distribution on the outer membrane surface obtained in this study might be influenced by the hollow fibre configuration with the microporous surface structure of kaolin support that was utilised as the support for photocatalyst TiO_2.

When a longer duration of hydrothermal reaction was applied, the deposition of TiO_2 nanorods on the outer membrane surface of kaolin support was expected to exhibit the increment in TiO_2 loading and the change in morphology of TiO_2 nanorods. By increasing the reaction time into 6 h and 10 h, the incremental loading of TiO_2 nanorods on the outer membrane surface was observed, resulting in the proper distribution of TiO_2 nanorods throughout the outer membrane surface as revealed in Fig. 4 **(a3)** and the immense deposition of TiO_2 nanorods on the outer membrane surface as seen in Fig. 4 **(a4)**. Meanwhile, the higher magnification of FESEM images in Fig. 4 **(b3)** and **(b4)** exposed that the hydrothermally synthesised TiO_2 nanorods were increased in size as a longer hydrothermal reaction time was used. By carrying out the hydrothermal reaction for 6 h and 10 h, the increase in average diameter of 0.69 μm and 0.74 μm and the decrease in average length of 3.97 μm and 3.04 μm were observed, respectively. The obtained results were in agreement with the study done by Liu and Aydil (2009), as they stated that the growth time was one of the factors that controlled both diameter and length of the hydrothermally grown TiO_2 nanorods. In addition, it was interesting to note that the hydrothermal reaction of 10 h could induce the formation of TiO_2 nanoflowers, in which TiO_2 nanorods were formed in flower-like arrangement on the outer membrane surface. This finding was in good agreement with the work conducted by Ahmad et al. (2016a) as they managed to obtain TiO_2 nanoflowers that grew on the top of TiO_2 nanorods array with thicker in size when a longer reaction time was used. So, the obtained result on the increase in average diameter, but the decrease in average length of TiO_2 nanorods might be attributed to the flower-like arrangement of TiO_2 nanorods.

Further examination on the effects of varying reaction times on the distribution of elements on the outer membrane surface were performed by EDX using the elemental mapping as shown in Fig. 5. The EDX analysis also provided a semi-quantitative chemical composition of kaolin/TNR membrane that prepared at different hydrothermal reaction times, as presented in Table 1. The existing elements found on the outer membrane surface of kaolin/TNR membrane that was prepared at 2 h and 6 h of hydrothermal reaction were Al and Si elements which represent the kaolin support, while O and Ti elements denoted the TiO_2 nanorods. By conducting the hydrothermal reaction for 2 h, only small amount of TiO_2 nanorods was formed on the outer membrane surface as proved by the low weight percentage of elements for TiO_2 nanorods shown in Table 1. Further observation on EDX mapping presented in Fig. 5 **(a2)** revealed that the outer surface of kaolin/TNR membrane was not uniformly distributed with TiO_2 nanorods, in which Ti and O elements were spotted at some parts of the outer membrane surface, resulting in the absence of TiO_2 layer with measurable thickness on the outer membrane surface observed in Fig. 3 **(b)**. However, by increasing the reaction duration into 6 h, the incline in weight percentage of elements for TiO_2 nanorods with the decline in weight percentage of elements for kaolin support were obtained, indicating the increase in loading of TiO_2 nanorods which resulted in the proper distribution of TiO_2 nanorods on the outer surface of kaolin/TNR membrane, as demonstrated by EDX mapping in Fig. 5 **(b2)** where more Ti and O elements were thoroughly scattered on the outer membrane surface.

When the hydrothermal reaction was performed in 10 h of reaction duration, the existing elements found on the outer surface of kaolin/TNR membrane were only Ti and O elements, as Al and Si

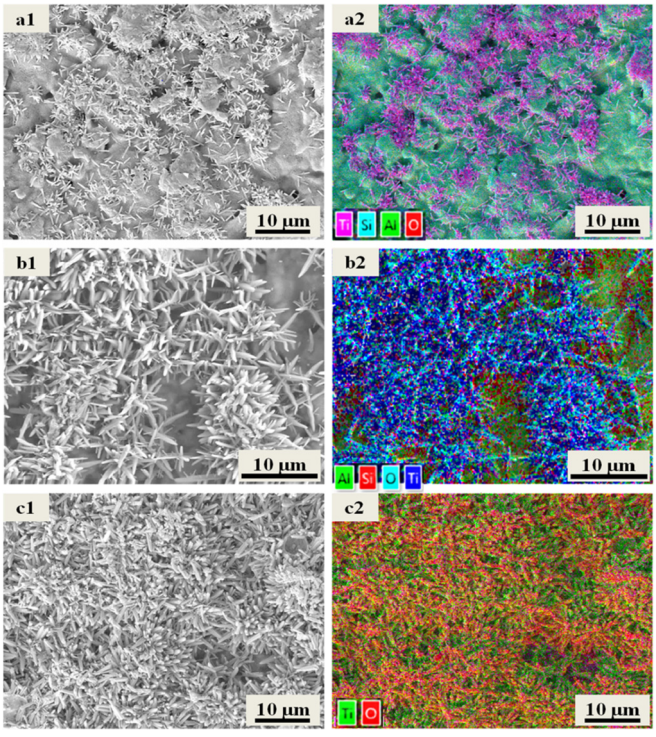

Fig. 5. (1) FESEM images and (2) EDX images of the outer surface of kaolin/TNR membrane that prepared at (a) 2 h, (b) 6 h, and (c) 10 h of reaction time.

Table 1
EDX chemical composition analysis for the outer surface of kaolin/TNR membrane.

Membrane sample	Element composition (wt%)			
	Al	Si	O	Ti
Kaolin/TNR membrane 2 h	18.3	17.2	35.7	27.4
Kaolin/TNR membrane 6 h	4.5	6.1	37.2	51.5
Kaolin/TNR membrane 10 h	–	–	47.0	52.8

elements were not detected by EDX analysis in Table 1, referring to Ti and O elements as the dominating elements found on the outer membrane surface with the further increment in their weight percentages. The obtained results indicated a further increase in loading of TiO_2 nanorods that resulted in the immense distribution of TiO_2 nanorods on the outer surface of kaolin/TNR membrane. The observation on EDX mapping in Fig. 5 **(c2)** emphasized that the outer surface of kaolin/TNR membrane were thoroughly covered with TiO_2 nanorods as no Al and Si elements were observed on the outer membrane surface, resulting in the formation of uniform TiO_2 layer with appropriate thickness on the outer membrane surface observed in Fig. 3 **(d)**. According to Nor et al. (2016), one of the crucial factors that ensured the excellent performance of photocatalytic membrane was the uniform distribution of TiO_2 photocatalysts on the top layer of membrane as they could be consistently exposed to the UV light during the photocatalytic degradation of target pollutants. So, based on the obtained results, the kaolin/TNR membrane that was prepared at 10 h of hydrothermal reaction was predicted to exhibit good photocatalytic performance due to high TiO_2 nanorods loading with the uniform distribution on the outer surface of kaolin/TNR membrane.

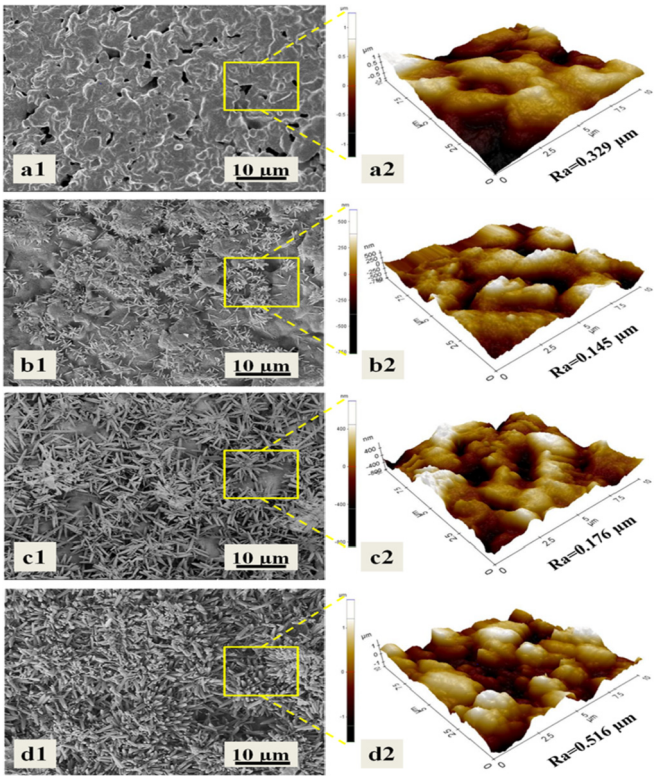

Fig. 6. (1) FESEM images and (2) AFM images of the outer surface of (a) kaolin support and kaolin/TNR membrane that prepared at (b) 2 h, (c) 6 h, and (d) 10 h of reaction time.

3.2. Surface structure and roughness of membrane

The effects of different hydrothermal reaction times on the membrane surface structure and roughness of kaolin/TNR membrane were examined by FESEM and AFM. As indicated by FESEM image in Fig. 6 **(a1)**, the membrane surface structure of kaolin support consisted of interconnected, plate-like grains and irregular pores that resulted from the grain growth mechanism of kaolin particles during the sintering process. In accordance with our previous work on kaolin hollow fibre membrane (Mohtor et al., 2017), the microporous structure for the outer membrane surface of kaolin support could be represented by high peaks (seen as bright regions) and deep depressions (seen as dark regions) that indicated the nodule-like aggregates and pores, respectively, as depicted by AFM image in Fig. 6 **(a2)**. By hydrothermally producing TiO_2 nanorods on the outer membrane surface in 2 h of reaction duration, the random deposition of TiO_2 nanorods on some parts of membrane surface was revealed by FESEM image in Fig. 6 **(b1)**, while the simultaneous incline in bright regions and decline in dark regions were observed in Fig. 6 **(b2)** that presented AFM image of the outer surface of kaolin/TNR membrane. These findings could be explained by the non-uniform distribution of TiO_2 nanorods on the microporous surface of kaolin support due to the shortest duration of hydrothermal reaction applied, resulting in the blockage of some pores with TiO_2 nanorods. Consequently, the surface structure of kaolin/TNR membrane became smoother with the mean surface roughness of 0.145 μm in comparison to the rougher surface of kaolin support with the mean surface roughness of 0.329 μm. The obtained results were in good agreement with the work done by Dzinun et al. (2015), as they highlighted that TiO_2/PVDF dual layer hollow fibre membrane possessed an outer surface that was smoother than its neat counterpart.

As the applied reaction time increased to 6 h and 10 h, the outer membrane surface of prepared membrane was thoroughly covered with the well deposition of TiO_2 nanorods, owing to the increase in TiO_2 loading along with the increase in length and diameter of TiO_2 nanorods as seen in Fig. 6 **(c1)** and along with the flower-like arrangement of TiO_2 nanorods as observed in Fig. 6 **(d1)**. The obtained results in FESEM images of the outer membrane surface of kaolin/TNR membrane that was prepared at 6 h and 10 h of hydrothermal reaction were in line with their AFM images, as demonstrated in Fig. 6 **(c2)** and **(d2)**, in which the intense formation in nodule-like aggregates of bright regions was observed due to the increase in formation of TiO_2 nanorods on the outer membrane surface as the longer reaction time was used. As a result, the increase in the mean surface roughness of kaolin/TNR membrane from 0.176 μm to 0.516 μm was obtained, along with the significant increment in the difference between high peak and low valley from 1.507 μm to 3.158 μm as presented in Table 2, which indicated that the rougher outer surface of kaolin/TNR membrane was observed due to the longer duration applied for the hydrothermal reaction. The similar trends in the incline of both mean surface roughness and the difference between high peak and low valley were also observed by Subramaniam et al. (2017), owing to the coarser surface of titanate nanotubes (TNT)/PVDF nanocomposite membrane with the higher TNT loading. Another similar result was also obtained by Mohamed et al. (2016) in their work on the preparation of regenerated cellulose (RC)/TiO_2 nanocomposite membrane with different TiO_2 loadings, as they indicated that the incline of TiO_2 nanorods resulted in the rougher surface of prepared membrane with the higher value in mean surface roughness.

3.3. Crystalline phases of membrane

The presence of crystalline phase of TiO_2 in prepared membrane

Table 2
Results of AFM analysis on the surface roughness parameters.

Membrane sample	Mean surface roughness, R_a (μm)	Root mean square roughness, R_q (μm)	Difference between high peak and low valley, R_z (μm)
Kaolin support	0.329	0.410	2.105
Kaolin/TNR membrane 2 h	0.145	0.185	1.367
Kaolin/TNR membrane 6 h	0.176	0.228	1.507
Kaolin/TNR membrane 10 h	0.516	0.614	3.158

was detected by XRD and XRD patterns of kaolin support and kaolin/TNR membrane that was prepared at different reaction times for hydrothermal process were demonstrated in Fig. 7. As observed in Fig. 7, all XRD patterns of kaolin/TNR membrane that was prepared at 2 h, 6 h, and 10 h of reaction times matched with XRD pattern of kaolin support with diffraction peaks detected at $2\theta = 16°$, 26°, 31°, 33°, 35°, 39°, 41°, 43°, 57°, 61° and 64°, which indicated mullite (Zhang et al., 2014) as the dominant crystalline phase presented in kaolin support due to the mullitisation of kaolinite that occurred at high sintering temperature of 1350 °C. These peaks for mullite were still detected in all XRD patterns of kaolin/TNR membrane due to the fact that the formation of TiO_2 layer on the outer membrane surface did not alter the crystalline structure of mullite in kaolin/TNR membrane. However, the intensities of these peaks decreased as the longer hydrothermal reaction time was used, owing to the higher loading of TiO_2 nanorods that was successfully deposited on the outer surface of kaolin/TNR membrane. As shown in Fig. 7 **(b)**, XRD pattern of kaolin/TNR membrane that was prepared at 2 h of hydrothermal reaction has an additional peak at $2\theta = 54°$ which corresponded to the [211] plane of rutile phase of TiO_2, indicating the limited formation of TiO_2 nanorods on the outer membrane surface in the shortest duration of hydrothermal process. This finding was in good agreement with the study conducted by Yusoff et al. (2016) in which the similar peak at $2\theta = 54°$ that represented the [211] plane of tetragonal rutile structure of TiO_2 nanorods was also obtained by using the growth time of 2 h.

By carrying out the hydrothermal reaction at 6 h, XRD pattern of kaolin/TNR membrane has three peaks at $2\theta = 36°$, 41°, and 54° that represented the [101], [111], and [211] planes of rutile phase of TiO_2 (PDF No. 00-021-1276) as depicted in Fig. 7 **(c)**. The presence of these peaks could be attributed by the formation of TiO_2 nanorods on the outer membrane surface with the increase in their length and diameter as the hydrothermal process was conducted at 6 h. The obtained result was in line with the observation on FESEM images of the outer surface of kaolin/TNR membrane in Fig. 4 **(a3)** and **(b3)**. On the other hand, as shown in Figure Fig. 7 **(d)**, there was an additional peak at $2\theta = 27°$ for XRD pattern of kaolin/TNR membrane that prepared at 10 h of reaction time, which corresponded the [110] plane of rutile phase of TiO_2. This peak indicated the formation of other nanostructure on the membrane surface, which was TiO_2 nanoflower that previously observed from FESEM images of the outer surface of kaolin/TNR membrane in Fig. 4 **(a4)** and **(b4)**. However, the obtained result in this study contradicted with the work carried out by Ahmad et al. (2016a) as they managed to observe the peak at $2\theta = 27°$ that corresponded to the [110] plane only by using 6 h of reaction time. Due to the fact that the nucleation process of TiO_2 nanoflowers only began by depositing on the tip of TiO_2 nanorods, the stable growth of TiO_2 nanoflowers was depended on the structure arrangement of TiO_2 nanorods. As a result, they easily obtained TiO_2 nanoflowers that grew on the glass substrate using the shorter reaction time since their work focused on the one-dimensional growth of TiO_2 nanorod array structure.

3.4. Functional groups of membrane

The presence of functional groups in kaolin/TNR membrane that resulted from varying the hydrothermal reaction duration was analysed by FTIR. From all FTIR spectra presented in Fig. 8, there was no significant difference observed in the absorption bands among them as all of them exhibited similar absorption bands at 1200-1000 cm^{-1} region that corresponded to the Si-O vibration of the amorphous silica (Ilic et al., 2010) and the bands at 850-650 cm^{-1} region that was attributed to the Al-O vibration of the mullite (Zhang et al., 2014). However, the obtained FTIR results would provide a complementary evidence in proving the presence of TiO_2 layer on the outer surface of kaolin/TNR membrane as

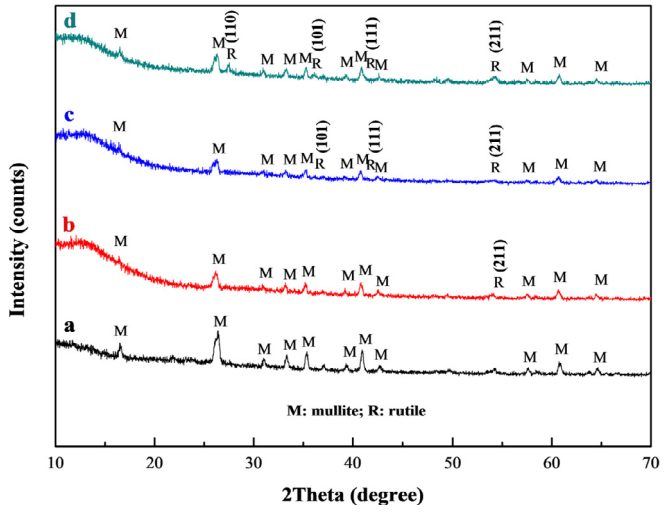

Fig. 7. XRD patterns of (a) kaolin support and kaolin/TNR membrane that was prepared at (b) 2 h, (c) 6 h, and (d) 10 h of reaction time.

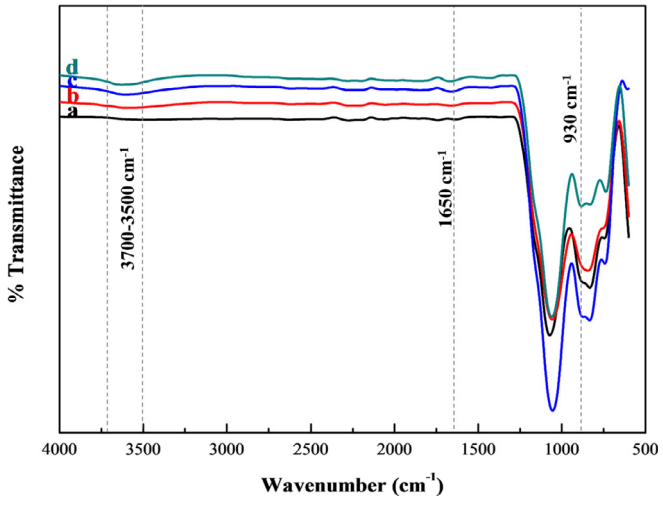

Fig. 8. FTIR spectra of (a) kaolin support and kaolin/TNR membrane that prepared at (b) 2 h, (c) 6 h, and (d) 10 h of reaction time.

observed in the previous FESEM and EDX images. As indicated by FTIR spectra in Fig. 8 **(b)**, **(c)**, and **(d)**, there were weak, yet noticeable broad bands observed at 3700-3500 cm^{-1} region and at around 1650 cm^{-1} that was assigned to the O-H stretching and bending vibrations of absorbed water (Mamulová Kutláková et al., 2011) on the outer surface of kaolin/TNR membrane. The intensities of these bands improved along with the increase in hydrothermal reaction time used, owing to the higher loading of TiO_2 nanorods that was distributed on the outer surface of kaolin/TNR membrane and thus, the more hydrogen bonds were formed between the absorbed water and TiO_2 nanorods on the outer membrane surface.

In this study, the formation of TiO_2 layer on the outer membrane surface was conducted by using the hydrothermal method that involved the chemical reactions as proposed by Cozzoli et al. (2003), in which TiO_2 nanorods were produced on the outer membrane surface of kaolin support through the chemical reactions that included both hydrolysis and condensation reactions, as illustrated in Fig. 9. During the hydrothermal process, the hydrolysis reaction firstly took place in which the four carbon atoms were eliminated from TBOT as the titanium precursor, in order to produce the titanium hydroxyl and the side-product of butanol. The formed titanium hydroxyl was consumed later in the condensation reaction in which TiO_2 was produced on the outer membrane surface when water was removed as the side-product. The produced TiO_2 in nanorod form was firmly adhered on the outer surface of kaolin/TNR membrane via the formation of Si-*O*-Ti chemical bonds, as there was a new band detected at 930 cm^{-1} in Fig. 8 that corresponded to Si-*O*-Ti bonding (Wang et al., 2011). The presence of these bonds should be preferable in ensuring the stable attachment of TiO_2 layer on the outer surface of kaolin/TNR membrane, particularly for its utilisation in the application of photocatalysis. Based on the FTIR spectra in Fig. 8, the band at 930 cm^{-1} became significantly apparent as the hydrothermal reaction time increased, indicating that the higher loading of TiO_2 nanorods would form additional hydrogen bonds with the absorbed water on the outer surface of kaolin/TNR membrane and thus, resulting in the improvement of surface affinity of kaolin/TNR towards water that should be highly beneficial for its usage in the water treatment applications.

3.5. Contact angle and water permeation of membrane

As one of the factors that influenced the water permeability of membrane, the surface hydrophilicity of membrane was analysed by using the contact angle measurement in order to investigate the

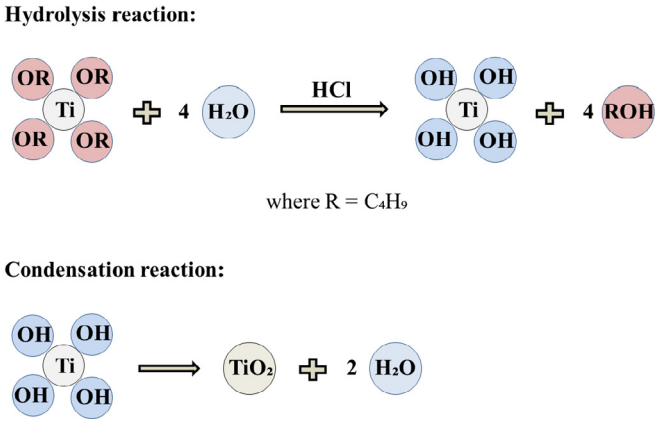

Fig. 9. Schematic illustration of reaction mechanism for the formation of TiO_2.

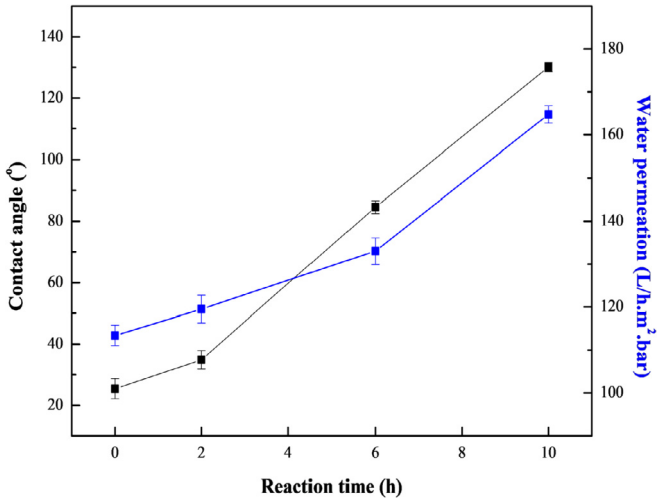

Fig. 10. Contact angle and water permeation of kaolin support and kaolin/TNR membrane that prepared at different reaction times.

effect of different hydrothermal reaction times on the hydrophilicity of membrane. From the obtained results on the contact angle that was depicted in Fig. 10, there was an incremental trend in the contact angle of membrane with an increment in the hydrothermal reaction time, indicating that the membrane surface became less hydrophilic as the longer reaction time was used. A similar finding was also demonstrated by Cao et al. (2006) in their work on the rutile TiO_2/PVDF membrane that exhibited the higher value in contact angle of 84° in comparison to the contact angle of 78° obtained by the PVDF membrane. Although TiO_2/PVDF membrane became more hydrophobic based on the obtained results on the contact angle measurement, they revealed that the rutile TiO_2/PVDF membrane had a higher water flux than its neat counterpart. So, from the obtained results on the contact angle of membrane, it could be stipulated that the hydrophilicity of membrane that was indicated by its contact angle was not the predominant factor that influenced the water permeability of membrane since according to Tan et al. (2017), the other contributing factors such as the liquid surface tension, the membrane surface charge, and the membrane surface roughness could also impose the change in membrane hydrophilicity. As a result, the increase in measured contact angle of kaolin/TNR membrane that was obtained in this work might be massively influenced by the incline in mean surface roughness of kaolin/TNR membrane when the longer reaction time was utilised, as revealed by the AFM images in Fig. 6.

The water permeation test was performed in order to investigate the the effects of varying hydrothermal reaction times on the performance of kaolin/TNR membrane and the result was presented in Fig. 10. According to the experimental results obtained, when the duration for hydrothermal process increased, the water permeation of prepared membrane was also enhanced accordingly, 113 ± 2.4 L/h.m^2.bar $<120 \pm 3.2$ L/h.m^2.bar $<133 \pm 3.1$ L/h.m^2.bar $<165 \pm 2.0$ L/h.m^2.bar. The increasing trend in the water permeation of the prepared membrane could be explained by the increasing loading of TiO_2 nanorods on the outer membrane surface as the longer reaction time was used for the hydrothermal process, resulting in the increment in the presence of hydroxyl functional groups on the outer surface of kaolin/TNR membrane that would easily promote the absorption of water molecules on the outer membrane surface. The improvement in the surface affinity of kaolin/TNR membrane towards water has enabled the high absorption of water molecules to permeate across the membrane, leading to the increment in water permeability of kaolin/TNR

membrane. In addition, the enhancement in water permeability of membrane was also contributed by the increase in surface roughness of membrane (Tan et al., 2017; Lai et al., 2016). From the obtained AFM images in Fig. 6, a rougher surface of kaolin/TNR membrane was observed as the longer reaction time was used, indicating the increase in effective surface area for water molecules to permeate through the membrane and thus, resulting in the improvement in water permeability of kaolin/TNR membrane.

3.6. Photocatalytic decolourisation of RB5

In order to examine the capability of membrane towards the adsorption of RB5, the adsorption of RB5 was performed on all prepared membranes in the dark condition for 180 min and the obtained results were depicted in Fig. 11. After 180 min of RB5 adsorption in the dark, the highest RB5 adsorption of 5.1% was attained by kaolin/TNR membrane was prepared at 10 h of hydrothermal reaction, followed by the adsorption values of 2.0% that were exhibited by kaolin/TNR membrane prepared at 6 h of hydrothermal reaction. The lowest RB5 adsorption was obtained by kaolin/TNR membrane prepared at 2 h of hydrothermal reaction and kaolin support with the same adsorption value of 0.8%. The differences in RB5 adsorption value obtained in this study might be explained by the differences in the effective surface area possessed by all prepared membrane. The highest RB5 adsorption that was attained by kaolin/TNR membrane prepared at 10 h of hydrothermal reaction was due to the formation of thickest TiO_2 layer on the outer membrane surface, owing to the highest TiO_2 loading with the excellent effective surface area on the outer membrane surface, which offered the high availability of active sites for the adsorption of RB5 molecules. This finding was in good agreement with the work done by Tahiri Alaoui et al. (2009) as they highlighted that the increase in active sites provided for the adsorption and degradation of pollution was highly dependent on the increment in photocatalyst loading.

Based on the RB5 adsorption in Fig. 11, it could be observed that all of the prepared membranes have achieved the steady state of RB5 adsorption in the dark within 100 min. The steady state of RB5 adsorption was said to be reached when no more RB5 molecules that being adsorbed or desorbed on the surface of photocatalyst and thus, the adsorption-desorption equilibrium was said to be achieved. Thus, the pre-equilibrium duration in the dark was determined at 100 min in order to ensure that the adsorption-desorption equilibrium occurred first before initiating the photocatalytic decolourisation of RB5 under UV irradiation. According to Nor et al. (2016), the good capability of membrane towards the adsorption of the pollutant's molecules would induce the promising result on the photocatalytic performance of membrane. Thus, among all the prepared kaolin/TNR membranes, the photocatalytic performance of kaolin/TNR membrane prepared at 10 h of hydrothermal reaction was predicted to exhibit good result in the decolourisation of RB5.

The photocatalytic efficiency of membrane was investigated by performing the photocatalytic decolourisation of RB5 under UV irradiation for 540 min and the obtained results were presented in Fig. 12. As revealed in Fig. 12 **(b)**, there was no appreciable decolourisation of RB5 exhibited by both direct photolysis and neat kaolin support since less than 1% RB5 decolourisation was achieved by them under UV exposure for 540 min. The obtained results might be explained by the stability of RB5 molecule due to its complex molecular structure with the presence of two azo N=N bonds, making the degradation of RB5 molecule was difficult to occur in the presence of UV light alone and in the absence of photocatalyst. Therefore, the direct photolysis of RB5 and the decolourisation of RB5 without the presence of photocatalyst could be considered as negligible in this work. The obtained results in this study were in line with the study done by You et al. (2012) as they observed the negligible degradation of RB5 by using the direct photolysis and the extremely low colour disappearance of RB5 by the neat PVDF membrane under the UV exposure for 120 min.

According to Fig. 12 **(b)**, all of the prepared kaolin/TNR membranes were able to exhibit RB5 colour disappearance steadily as a function of the UV irradiation time due to the presence of UV/TiO_2 system in the heterogeneous photocatalysis of RB5. However, the kaolin/TNR membrane that was prepared at 2 h of hydrothermal reaction could hardly photodegrade RB5 molecule due to the lowest TiO_2 loading on the outer membrane surface, resulting in a negligible RB5 decolourisation of 1.7%. In contrast, the highest RB5 decolourisation of 80.3% was demonstrated by kaolin/TNR

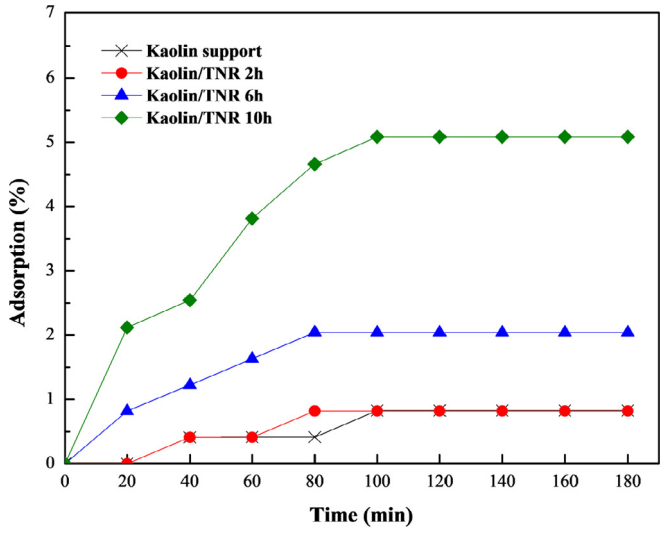

Fig. 11. RB5 adsorption of prepared membranes in dark conditions.

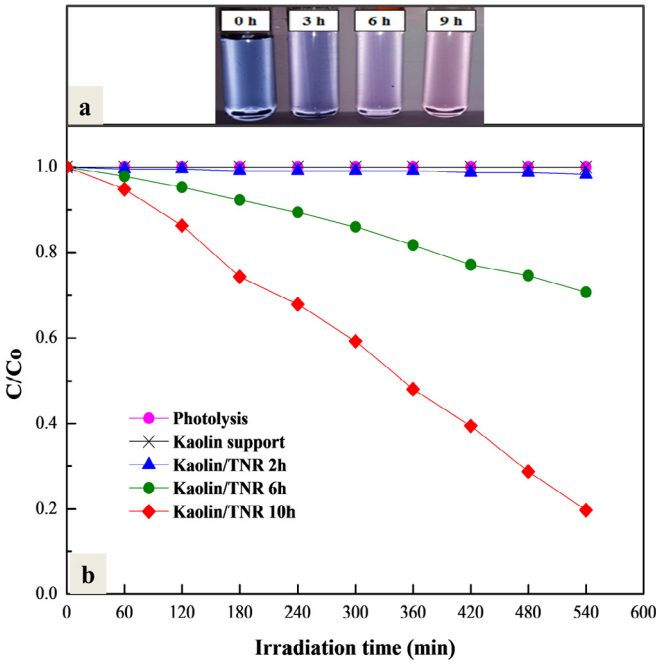

Fig. 12. (a) Visible colour change of RB5 by of kaolin/TNR membrane that prepared at 10 h of hydrothermal reaction, (b) Photocatalytic performance of kaolin/TNR membranes under UV irradiation.

membrane that was prepared at 10 h of hydrothermal reaction, followed by 29.4% RB5 decolourisation that was attained by kaolin/TNR membrane prepared by conducting hydrothermal reactions for 6 h. The obtained results could be explained by the highest loading of TiO_2 nanorods on the outer surface of kaolin/TNR membrane that was prepared at 10 h of hydrothermal reaction, allowing more effective surface area of TiO_2 to be easily accessible for the absorption of photon in order to induce the photocatalyst activation. As a result, the reactive hydroxyl radicals were generated under UV irradiation that was responsible for the degradation of most of RB5 molecules presented in the feed solution, resulting in the highest RB5 decolourisation that was achieved by kaolin/TNR membrane prepared at 10 h of hydrothermal reaction.

The photocatalytic degradation of RB5 in UV/TiO_2 system usually involved the oxidation on both of azo N=N bonds by hydroxyl radicals, resulting in the decolourisation and mineralisation of RB5. However, the focus in this work was only on the decolourisation of RB5 since the complete mineralisation of RB5 has been detailed elsewhere (Zhou et al., 2016). In order to further confirm the RB5 decolourisation by kaolin/TNR membrane, the observation on visible colour changes of RB5 in the feed solution was performed. As revealed by the colour changes of RB5 that was exhibited by the collected feed samples at specific time interval in Fig. 12 **(a)**, the kaolin/TNR membrane prepared from 10 h of hydrothermal reaction has successfully reduced the colour intensity of RB5 from the dark navy blue to the light pink after 540 min of UV exposure, which corresponded to the achievement of 80.3% RB5 decolourisation. The reduction in colour intensity of RB5 observed in this work could be attributed to the cleavage of bonds for the colour giver group of chromophore in RB5 molecule, resulting in the decolourisation of RB5 (Zhou et al., 2016; Nasuha et al., 2016).

The photocatalytic performance of kaolin/TNR membrane prepared by the hydrothermal reaction for 10 h was compared with previous works on the dye degradation using TiO_2 under various controlled parameters. As shown in Table 3, the obtained result on RB5 degradation from this study was comparable to other studies that focused on the application of immobilised TiO_2 on support in the photocatalytic reactor system. Although the suspended TiO_2 generally possessed a higher photocatalytic activity in the dye degradation, it commonly faced recovery problems from the treated solution after UV irradiation. In contrast, the recovery of suspended TiO_2 from the treated solution was much easier, favouring the reusability of suspended TiO_2 in the subsequent cycles of photocatalytic reaction.

The reusability of fabricated kaolin/TNR membrane was also evaluated by recycling the membrane over three consecutive cycles in the photocatalytic decolourisation of RB5. In this reusability experiment, the kaolin/TNR membrane prepared by the hydrothermal reaction for 10 h was selected since it displayed the highest photocatalytic activity in RB5 decolorization. At the end of each cycle, the membrane was washed several times with distilled water and dried at 60 °C. As shown in Fig. 13, the kaolin/TNR membrane demonstrated negligible reduction in photocatalytic decolourisation of RB5 after repeated usage after three consecutive regeneration cycles, indicating that it was fairly stable and did not undergo significant photocorrosion during the photocatalytic decolorization of RB5 under UV irradiation. The similar finding were also attained by previous work on the immobilised TiO_2 by Tao et al. (2016) for the four consecutive cycles of photocatalytic degradation of methyl orange (MO). The excellent stability of kaolin/TNR membrane could enable it to be reused for several cycles of photocatalytic reactions without reducing the photocatalytic efficiency of kaolin/TNR membrane, thus making it to be a cost-effective choice of photocatalytic ceramic membrane for the degradation of pollutants under UV exposure.

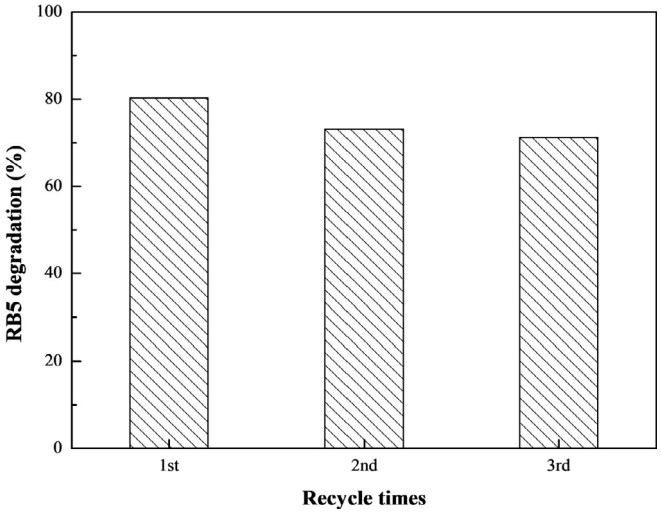

Fig. 13. Regeneration efficiency of kaolin/TNR membrane prepared at 10 h of hydrothermal reaction for three consecutive cycles.

4. Conclusion

The kaolin support has been successfully deposited with TiO_2 layer on the outer membrane surface for the preparation of kaolin/TNR membrane by using hydrothermal method. By varying the hydrothermal reaction times, the increasing duration for hydrothermal reaction could impose the incremental TiO_2 loading with the uniform distribution on the outer membrane surface, resulting in the formation of thicker TiO_2 layer and rougher outer surface of kaolin/TNR membrane. From the obtained characterisation results, it was found that the highest TiO_2 loading with the excellent effective surface area on the outer membrane surface had resulted in the highest water permeation of 165 L/h.m^2.bar that was

Table 3
Comparison of dye degradation with previous studies.

Dye	Photocatalyst	Initial concentration	Light source	Time	Degradation (%)	Reference
Methyl orange	Immobilised TiO_2 (TNRs)	15 ppm	High pressure mercury lamp (36 W)	100 min	82	(Tao et al., 2016)
RB5	Suspended TiO_2 (P25)	250 ppm	Low pressure UV lamp (75 W)	240 min	100	(Tang and Chen, 2004)
RB5	Suspended TiO_2 (NPs)	10 ppm	UV lamp	150 min	97	(Chong et al., 2015)
RB5	Immobilised TiO_2 (NPs)	40 ppm	UV lamp (15 W)	120 min	42	(You et al., 2012)
RB5	Immobilised TiO_2 (TNRs)	10 ppm	UVA lamp (36 W)	360 min	52	Present work

exhibited by kaolin/TNR membrane prepared from 10 h of hydrothermal reaction. As a result, among all kaolin/TNR membranes that was prepared by using hydrothermal method, the highest RB5 decolourisation of 80.3% was also obtained by the kaolin/TNR membrane prepared at hydrothermal reaction of 10 h. As a conclusion, the reaction time of 10 h has been selected as the most suitable duration for hydrothermal reaction in order to prepare kaolin/TNR membrane with uniform distribution of TiO_2 layer on the outer membrane surface that improved the membrane performance in both water treatment application and photocatalytic reaction.

Acknowledgement

The authors gratefully acknowledge the financial support from the Ministry of Education Malaysia under the Higher Institution Centre of Excellence Scheme (Project Number: R.J090301.7846.4J192), Universiti Teknologi Malaysia under the Research University Grant Tier 1 (Project number: Q.J130000.2546.16H40). The authors would also like to thank the Research Management Centre, Universiti Teknologi Malaysia for their technical support.

References

Ahmad, M.K., Mokhtar, S.M., Soon, C.F., Nafarizal, N., Suriani, A.B., Mohamed, A., Mamat, M.H., Malek, M.F., Shimomura, M., Murakami, K., 2016. Raman investigation of rutile-phased TiO_2 nanorods/nanoflowers with various reaction times using one step hydrothermal method. J. Mater. Sci. Mater. Electron. 27, 7920–7926.

Ahmad, M.K., Soon, C.F., Nafarizal, N., Suriani, A.B., Mohamed, A., Mamat, M.H., Malek, M.F., Shimomura, M., Murakami, K., 2016. Effect of heat treatment to the rutile based dye sensitized solar cell. Optik 127, 4076–4079.

Bouzerara, F., Harabi, A., Achour, S., Larbot, A., 2006. Porous ceramic supports for membranes prepared from kaolin and doloma mixtures. J. Eur. Ceram. Soc. 26, 1663–1671.

Cao, X., Ma, J., Shi, X., Ren, Z., 2006. Effect of TiO_2 nanoparticle size on the performance of PVDF membrane. Appl. Surf. Sci. 253, 2003–2010.

Cao, C., Hu, C., Wang, X., Wang, S., Tian, Y., Zhang, H., 2011. UV sensor based on TiO_2 nanorod arrays on FTO thin film. Sensor. Actuator. B Chem. 156 (1), 114–119.

Chang, J.H., Ellis, A.V., Hsieh, Y.H., Tung, C.H., Shen, S.Y., 2009. Electrocatalytic characterization and dye degradation of nano-TiO_2 electrode films fabricated by CVD. Sci. Environ 407, 5914–5920.

Chong, M.N., Cho, Y.J., Poh, P.E., Jin, B., 2015. Evaluation of titanium dioxide photocatalytic technology for the treatment of reactive black 5 dye in synthetic and real greywater effluents. J. Clean. Prod. 89, 196–202.

Cozzoli, P.D., Kornowski, A., Weller, H., 2003. Low-temperature synthesis of soluble and processable organic-capped anatase TiO_2 nanorods. J. Am. Chem. Soc. 125, 14539–14548.

Damodar, R.A., You, S.J., Chou, H.H., 2009. Study the self cleaning, antibacterial and photocatalytic properties of TiO_2 entrapped PVDF membranes. J. Hazard Mater. 172, 1321–1328.

Dzinun, H., Othman, M.H.D., Ismail, A.F., Puteh, M.H., Rahman, M.A., Jaafar, J., 2015. Morphological study of co-extruded dual-layer hollow fiber membranes incorporated with different TiO_2 loadings. J. Membr. Sci. 479, 123–131.

Faisal, A.Q.D., 2015. Synthesis and characteristic study of TiO_2 nanowires and nanoflowers on FTO/glass and glass substrates via hydrothermal method. J. Mater. Sci. Mater. Electron. 26, 317–321.

Harabi, A., Zenikheri, F., Boudaira, B., Bouzerara, F., Guechi, A., Foughali, L., 2014. A new and economic approach to fabricate resistant porous membrane supports using kaolin and $CaCO_3$. J. Eur. Ceram. Soc. 34, 1329–1340.

Ilic, B.R., Mitrovic, A.A., Milicic, L.R., 2010. Thermal treatment of kaolin clay to obtain metakaolin. Hem. Ind. 64, 351–356.

Jiu, J., Wang, F., Adachi, M., 2004. Preparation of highly photocatalytic active nanoscale TiO_2 by mixed template method. Mater. Lett. 58, 3915–3919.

Lai, G.S., Lau, W.J., Goh, P.S., Ismail, A.F., Yusof, N., Tan, Y.H., 2016. Graphene oxide incorporated thin film nanocomposite nanofiltration membrane for enhanced salt removal performance. Desalination 387, 14–24.

Leong, S., Razmjou, A., Wang, K., Hapgood, K., Zhang, X., Wang, H., 2014. TiO_2 based photocatalytic membranes: a review. J. Membr. Sci. 472, 167–184.

Lin, Y.F., Tung, K.L., Tzeng, Y.S., Chen, J.H., Chang, K.S., 2012. Rapid atmospheric plasma spray coating preparation and photocatalytic activity of macroporous titania nanocrystalline membranes. J. Membr. Sci. 389, 83–90.

Linsebigler, A.L., Lu, G., Yates Jr., J.T., 1995. Photocatalysis on TiO_2 surfaces: principles, mechanisms, and selected results. Chem. Rev. 95 (3), 735–758.

Liu, B., Aydil, E.S., 2009. Growth of oriented single-crystalline rutile TiO_2 nanorods on transparent conducting substrates for dye-sensitized solar cells. J. Am. Chem. Soc. 131, 3985–3990.

Mamulová Kutláková, K., Tokarský, J., Kovář, P., Vojtěšková, S., Kovářová, A., Smetana, B., Kukutschová, J., Čapková, P., Matějka, V., 2011. Preparation and characterization of photoactive composite kaolinite/TiO_2. J. Hazard Mater. 188, 212–220.

Mohamed, M.A., Salleh, W.N.W., Jaafar, J., Ismail, A.F., Mutalib, M.A., Sani, N.A.A., Asri, S.E.A.M., Ong, C.S., 2016. Physicochemical characteristic of regenerated cellulose/N-doped TiO_2 nanocomposite membrane fabricated from recycled newspaper with photocatalytic activity under UV and visible light irradiation. Chem. Eng. J. 284, 202–215.

Mohtor, N.H., Othman, M.H.D., Ismail, A.F., Rahman, M.A., Jaafar, J., Hashim, N.A., 2017. Investigation on the effect of sintering temperature on kaolin hollow fibre membrane for dye filtration. Environ. Sci. Pollut. Res. 24, 15905–15917.

Nasuha, N., Ismail, S., Hameed, B.H., 2016. Activated electric arc furnace slag as an efficient and reusable heterogeneous Fenton-like catalyst for the degradation of Reactive Black 5. J. Taiwan Inst. Chem. Eng 67, 235–243.

Nor, N.A.M., Jaafar, J., Ismail, A.F., Mohamed, M.A., Rahman, M.A., Othman, M.H.D., Lau, W.J., Yusof, N., 2016. Preparation and performance of PVDF-based nanocomposite membrane consisting of TiO_2 nanofibers for organic pollutant decomposition in wastewater under UV irradiation. Desalination 391, 89–97.

Okuya, M., Shiozaki, K., Horikawa, N., Kosugi, T., Kumara, G.R.A., Madarasz, J.A., Kaneko, S., Pokol, G., 2004. Porous TiO_2 thin films prepared by spray pyrolysis deposition (SPD) technique and their application to UV sensors. Solid State Ionics 172 (1–4), 527–531.

Sarbatly, R., 2011. Effect of kaolin/pesf ratio and sintering temperature on pore size and porosity of the kaolin membrane support. J. Appl. Sci. 11 (13), 2306–2312.

Song, M.Y., Kim, D.K., Jo, S.M., Kim, D.Y., 2005. Enhancement of the photocurrent generation in dye-sensitized solar cell based on electrospun TiO_2 electrode by surface treatment. Synth. Met. 155, 635–638.

Subramaniam, M.N., Goh, P.S., Lau, W.J., Tan, Y.H., Ng, B.C., Ismail, A.F., 2017. Hydrophilic hollow fiber PVDF ultrafiltration membrane incorporated with titanate nanotubes for decolourization of aerobically-treated palm oil mill effluent. Chem. Eng. J. 316, 101–110.

Tahiri Alaoui, O., Nguyen, Q.T., Mbareck, C., Rhlalou, T., 2009. Elaboration and study of poly(vinylidene fluoride)–anatase TiO_2 composite membranes in photocatalytic degradation of dyes. Appl. Catal., A 358, 13–20.

Tan, Y.H., Goh, P.S., Ismail, A.F., Ng, B.C., Lai, G.S., 2017. Decolourization of aerobically treated palm oil mill effluent (AT-POME) using polyvinylidene fluoride (PVDF) ultrafiltration membrane incorporated with coupled zinc-iron oxide nanoparticles. Chem. Eng. J. 308, 359–369.

Tang, C., Chen, V., 2004. The photocatalytic degradation of reactive black 5 using TiO_2/UV in an annular photoreactor. Water Res. 38, 2775–2781.

Tao, J., Gong, Z., Yao, G., Cheng, Y., Zhang, M., Lv, J., Shi, S., He, G., Chen, X., Sun, Z., 2016. Hydrothermal growth of nanorod arrays and in situ conversion to nanotube arrays for highly efficient Ag-sensitized photocatalyst. J. Alloy. Comp. 689, 451–459.

Wang, C., Shi, H., Zhang, P., Li, Y., 2011. Synthesis and characterization of kaolinite/TiO_2 nano-photocatalyst. Appl. Clay Sci. 53, 646–649.

Xiong, J., Yang, B., Yuan, J., Fan, L., Hu, X., Xie, H., Lyu, L., Cui, R., Zou, Y., Zhou, C., Niu, D., Gao, Y., Yang, J., 2015. Efficient organic photovoltaics using solution-processed, annealing-free TiO_2 nanocrystalline particles as an interface modification layer. Org. Electron. 17, 253–261.

You, S.J., Semblante, G.U., Lu, S.C., Damodar, R.A., Wei, T.C., 2012. Evaluation of the antifouling and photocatalytic properties of poly(vinylidene fluoride) plasma-grafted poly(acrylic acid) membrane with self-assembled TiO_2. J. Hazard Mater. 237–238, 10–19.

Yuan, Z.Y., Su, B.L., 2004. Titanium oxide nanotubes, nanofibers and nanowires, Colloids Surf. A: Physicochem. Eng. Aspects 241, 173–183.

Yusoff, M.M., Mamat, M.H., Malek, M.F., Suriani, A.B., Mohamed, A., Ahmad, M.K., Alrokayan, S.A.H., Khan, H.A., Rusop, M., 2016. Growth of titanium dioxide nanorod arrays through the aqueous chemical route under a novel and facile low-cost method. Mater. Lett. 164, 294–298.

Zhang, Y., Gao, Y., Xia, X.H., Deng, Q.R., Guo, M.L., Wan, L., Shao, G., 2010. Structural engineering of thin films of vertically aligned TiO_2 nanorods. Mater. Lett. 64 (14), 1614–1617.

Zhang, Z., Qiao, X., Yu, J., 2014. Microwave selective heating-enhanced reaction rates for mullite preparation from kaolinite. RSC Adv. 4, 2640–2647.

Zhou, K., Hu, X.Y., Chen, B.Y., Hsueh, C.C., Zhang, Q., Wang, J., Lin, Y.J., Chang, C.T., 2016. Synthesized TiO_2/ZSM-5 composites used for the photocatalytic degradation of azo dye: intermediates, reaction pathway, mechanism and biotoxicity. Appl. Surf. Sci. 383, 300–309.